Ceramics International **21** (1995) 283–287

Covalent Bonding in MgO and Y_2O_3

Ľubomír Benco

Institute of Inorganic Chemistry, Slovak Academy of Sciences, Dúbravská cesta 9, 842 36 Bratislava, Slovak Republic

(Received 11 November 1994; accepted 14 December 1994)

Abstract: The electronic structure of sintering aids is studied using extended Hückel tight-binding method. The chemical bonding is compared and contrasted for MgO and Y_2O_3. The covalency degree is evaluated in terms of the metal orbital admixture to the bands of occupied states. This was found to be approximately twice as large for Y_2O_3 compared with MgO. The influence of the covalent interaction on the shape of the occupied bands is demonstrated for valence bands resulting in its two peak structure for both oxides. The band composition analysis shows increased directional character of the chemical bonding in Y_2O_3 compared with MgO.

1 INTRODUCTION

Both oxides, MgO and Y_2O_3, belong to the group of sintering aids commonly used in a process of joining grains of Si_3N_4. They create a grain boundary liquid phase wetting grain surfaces, thus producing dense ceramics. This liquid phase mediates effective chemical bonding between grains and grain boundary phase. Though both oxides are highly stable and refractory compounds, the melting temperature of the eutectic grain boundary alloy is relatively low. The presence of the grain boundary phase always deteriorates high temperature mechanical properties of the ceramics. Additional kinds of chemical bonds appearing at grain boundaries represent one of the reasons for this phenomenon. While a single crystal of Si_3N_4 contains only Si–N bonds, in the sintered material Si–O and M–O bonds are also embodied (M stands for the metal atom of the sintering aid). Oxygen atoms taking part in bonds at grain boundaries come either from oxide or from environmental oxygen overlying grain surfaces.[1,2] Both Si–N and Si–O bonds are known to be highly covalent. The M–O bond, on the contrary, represents a new feature influencing mechanical properties of the sintered material. Though these bonds are highly ionic for both metals, magnesium and yttrium, pronounced differences exist in their degree of covalency. The band structure of MgO has been studied by various methods[3–15,33] and is reasonably well established. On the contrary, the first papers reporting on the band structure of Y_2O_3 appeared only recently.[16,17]

In the present work the metal-to-oxygen bonding is compared and contrasted for the stoichiometric crystals MgO and Y_2O_3. The paper is organized as follows: in Section 2 a brief outline of the method of calculation is followed by details on structures of the two crystals. Results are presented in Section 3 in the form of density of states (DOS). The degree of covalency is evaluated through the analysis of the band composition. Some discussion of the directional properties of the metal-to-oxygen bonding is completed with concluding remarks made in the last section

2 METHOD OF CALCULATION

Extended Hückel[18] (EHT) tight-binding calculations[19,20,34] are performed. For MgO the crystal structure data from the single crystal determination by Sasaki *et al.*[21] are used. MgO has a rock salt-type structure (space group symmetry *Fm3m*; the cell parameter a = 4·217 Å). It consists of interpenetrating fcc lattices of Mg and O ions, each atom having an octahedral surrounding of atoms of the opposite species. Yttria crystallizes in a very complicated bixbyite structure (space group symmetry *Ia*3; the cell parameter a = 10·604 Å) in

Table 1. Orbital parameters used in band structure calculations

Atom	Orbital	H_{ii}(eV)	$\zeta_{i1}(c_1)$	$\zeta_{i2}(c_2)$
O[1]	2s	-32·30	2·275	
	2p	-14·80	2·275	
Mg[1]	3s	-9·00	1·100	
	3p	-4·50	1·100	
Y[2]	4d	-6·80	3·550(0·3041)	1·560(0·8316)
	5s	-7·02	1·740	
	5p	-4·40	1·700	

[1]From *Table of Parameters for Extended Hückel Calculations*; collected by Santiago Alvarez, Barcelona, 1985.
[2]Ref. 25. H_{ii}, orbital ionization energies; ζ_{ij}, Slater exponents, c_j, coefficients in the double-zeta expansion of the d orbitals.

which the cubic cell contains sixteen molecules.[22] According to structural data from the X-ray Rietveld powder refinement[23] the Y–O bond lengths range from 2·22 to 2·32 Å. In a simplified picture one may think of the Y atom as being in a highly distorted octahedral environment, while the O atom has a distorted tetrahedral coordination.

Table 1 summarizes the extended Hückel parameters used. The solid state calculation for both oxides are performed using 56 **k** points uniformly distributed in the irreducible wedge of the Brillouin zone.[24]

3 RESULTS AND DISCUSSION

3.1 Density of states

Energy levels sampled in a set of **k** points result in the DOS curves shown in Fig. 1. The states are grouped into three bands separated by energy

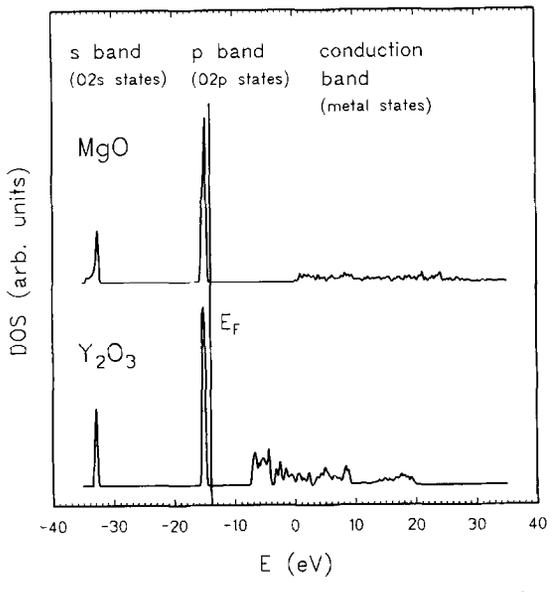

Fig. 1. The total DOS curves for MgO and Y_2O_3 showing energy levels in the valence region. The states below the Fermi level (E_F) are occupied, the conduction band represents empty states.

gaps, two of them being situated bellow the Fermi level (E_F). Because of the close positions of the E_F (≈–14·2 eV and ≈–14·3 eV for MgO and Y_2O_3, respectively) this level is for both oxides indicated by a single vertical line. The bands of occupied states (s and p band) are narrow. On the contrary, the conduction band (CB) on the right of Fig. 1 is comprised of unoccupied nonbonding states dispersed over a large energy range. The bands of occupied states measured experimentally are broader, e.g. the total width of the valence band (VB) for MgO is about 6 eV.[26,27] Nevertheless, it must be noted that ceramic oxides are usually contaminated with defects and impurities causing the band broadening which is very difficult to distinguish. Though the methodology used in the present work is approximate it provides a conceptual basis for understanding the chemical bonding.[28] In both oxides the Fermi level falls at the edge of the valence band. Such a configuration with closed energy bands documents high stability of the system. Broad energy gaps between the VB and the CB, responsible for their insulating properties, enable the refractory behaviour of these materials. The highly ionic character of the metal-to-oxygen bond means that almost all of the metal atom valence electrons are transferred to oxygen atoms. The high electronegativity of the oxygen atoms and the large energy difference between atomic O 2s and O 2p energy levels cause a separation of the corresponding energy states. Thus in both oxides the O 2s states dominate in the s band and O 2p states in the p band. The unoccupied states of the CB consist almost entirely of metal s and p orbitals in MgO, completed with empty d orbitals in Y_2O_3. The states of d orbitals taking part in the chemical bonding of transition metal (TM) oxides greatly influence their properties. In Y_2O_3 empty d states are located in the upper part of the energy gap (Fig. 1) thus lowering its value compared with the band gap of MgO. On the other hand, the smaller energy difference between the atomic energy levels enables increased O 2p–Y 3d interaction. Further details on the metal-to-oxygen hybridization are given in Section 3.3. The band gap lowering in Y_2O_3 corresponds to the decreasing of its melting point to the value 2420°C, compared with the value 2820° for MgO.

3.2 Shape of the valence band

The metal orbital admixture to the s and p bands influences the shape of the bands. This admixture results from the overlap of AOs. The states due to the covalent component of the bond are stabilized compared with the ionic component, i.e. they are

shifted to the higher binding energies (more negative energies). The mechanism of the stabilization through the covalent interaction is the same for both bands of occupied states. Figure 2 shows details for the valence band where the covalent admixture is more pronounced. The total DOS curve for MgO and Y_2O_3 is shown together with the partial DOS coming from the metal atoms. Both systems show the two peak structure of the valence band. The first peak is situated at ≈–14·8 eV, representing the states of the lone electron pairs on oxygen atoms. The second peak, shifted by some 0·5 eV towards higher binding energies, represents the covalent part of the bonding. It corresponds well with a maximum of the partial metal DOS admixture. In Y_2O_3 the contribution of the partial metal DOS to the valence band is much higher than in MgO and the total DOS consists of two components of comparable intensity. Note that the small admixture of the metal states raises the stabilization of oxygen 2p states (further details are given in Section 3.3). Though Ching and Xu[16] do not discuss the iono-covalent properties of the chemical bonding in Y_2O_3 their first-principle total and partial DOS agree well with results presented in this work. Similarly, the cluster calculation on Y_2O_3 reported by Jollet *et al.*,[17] though complicated by finite-size effects, comes to the same two-peak structure of the VB. As the DOS should be compared with the photoemission spectra the comparison is given in Fig. 3. The measured VB spectra show a single major peak. Two total DOS curves (Fig. 3, curves b and c) are shifted towards the band centre of gravity in order to be aligned with the VB DOS and the major peak of the XPS spectra. This shift is fully justified as the DOS is

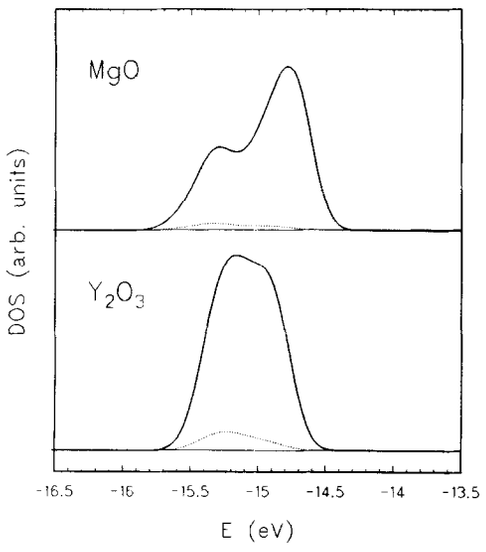

Fig. 2. The total DOS curves (full line) for the valence band completed with the partial metal DOS (dotted line). The metal orbital admixture corresponds with the covalency degree of the chemical bonding.

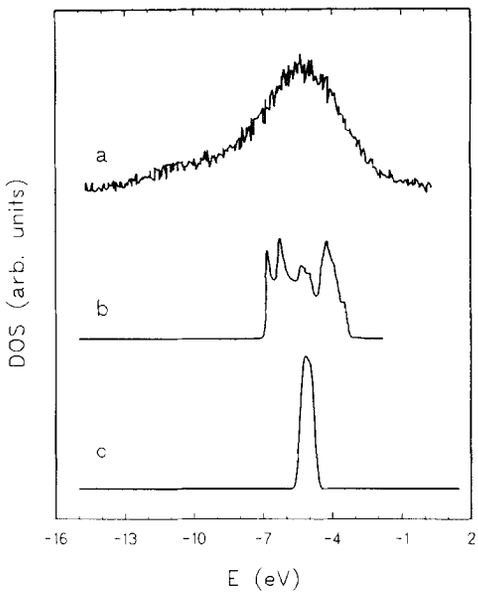

Fig. 3. The shape of the valence band as obtained by the photoemission spectroscopy (a),[17] first-principles OLCAO method (b),[16] and EHT method (c, this work). Both theoretical curves demonstrate the fact that deep lying states at ≈–11 eV cannot originate in the ideal structure of Y_2O_3 (see text).

obtained for the ideal crystal and the measured Fermi level position is moved upwards due to surface states. The comparison shows that the main XPS peak comprises both VB components, and also the states due to the ionic and the covalent bonding, the latter states being responsible for the higher energy part of the photoemission curve. The small intensity tail extending to more than 10 eV cannot originate in the VB of the ideal structure of Y_2O_3. Haruyama *et al.*[29] in their XPS study on $SrTiO_3$ (100) have shown recently that states approximately 11 eV below the Fermi level are closely connected with oxygen vacancies near the surface. In the light of their findings we support the view of Ching and Xu[16] that the low-intensity peak comes from the defect-related structure rather than the intrinsic VB states in Y_2O_3. Moreover, the spectra were recorded on samples manufactured by the sintering process[17] supporting the oxygen vacancy creation.

3.3 Degree of covalency

Covalent and ionic bonds differ from each other in the valence charge density distribution. In the covalent bond the valence charge density is shared by the neighbouring atoms and its maximum is situated between the atomic nuclei. On the other hand, in the ionic bond the valence charge density is located around the more electronegative atom. Closed atomic levels (completely filled or emptied for the electronegative or electropositive atom, respectively) result in the spherical distribution of

Table 2. Band composition for MgO and Y_2O_3

	Atom	Orbital	Content (%) s band	Content (%) p band
MgO	Mg	3s	9·07	1·59
		3p	0·15	2·77
	O	2s	90·78	0·06
		2p	0·0	95·58
Y_2O_3	Y	5s	2·45	1·26
		5p	2·23	2·30
		4d	4·75	4·48
	O	2s	90·57	0·01
		2p	0·0	91·95

the charge density. This is the reason why structures of ionic compounds are simpler than structures of covalent systems. The charge transfer occurring in the process of the bond creation is usually characterized by the effective atomic charge. This single number reflects the global charge density distribution and corresponds to the degree of ionicity (or covalency). According to the highly precise first-principles computational OLCAO procedure,[15,16] magnesia and yttria should be described as $Mg^{+1\cdot83}O^{-1\cdot83}$ and $Y_2^{+2\cdot16}O_3^{-1\cdot44}$. These formulae show that both oxides are far from being ideal ionic compounds, yttria showing a considerable degree of covalency. The increasing role of the metal orbitals in the chemical bonding necessitates careful analysis of the atomic level occupation. The composition of bands for the occupied states is given in Table 2. Both bands show differences for the two oxides. Let us discuss the s band first. Though the metal atom admixture to the band is similar (9·22 and 9·43% for MgO and Y_2O_3, respectively) the occupation of the metal atom energy levels differs. In MgO almost the whole metal contribution comes from spherical s orbitals. On the contrary, in Y_2O_3 the occupation of the p states is comparable to the number of the occupied s states and the number of d states is almost twice as large as the s state occupation. The p band represents the outer valence region forming the shape of the bonding charge density distribution. The number of its states is three times larger than that of the s band (see Fig. 1). The properties of materials depending on the chemical bonding correlate with the outer valence band composition. In the p band the occupation of the s and p levels is similar in both oxides. Nevertheless, in Y_2O_3 the metal orbital admixture is due to the d orbitals being almost twice as large compared with MgO. The effective inclusion of the d orbitals into the chemical bonding changes the character of the interatomic interaction. The M–O bonds become more covalent, i.e. a part of the electron density is transferred from oxygen atoms towards metal atoms. The increased covalency is reflected in different mechanical properties (e.g. the strength increases from 100 MPa for MgO to 290 MPa for Y_2O_3[30]). The charge density distribution is no longer spherical but shaped according to the directional characteristics of the d orbitals. Though an increased degree of covalency causes improved mechanical properties which are, in sintering aids, highly desirable, the directional character of the interatomic interaction brings difficulties into the process of creating bonds at grain boundaries. The degree of covalency of the Mg–O bond is considerably lower compared with Y–O. The interaction of Mg to oxygen atoms resembles the interaction of spherical particles. The coordination of the magnesium atom is thus not restricted to some kind of polyhedra. Consequently, in the process of creating chemical bonds at grain boundaries, Mg atoms support the formation of the amorphous intergranular phase and MgO performs as an outstanding sintering aid.[31,32] On the contrary, the increased covalency of the Y–O bond, documented in Table 2, means that yttrium atoms, when coordinated by oxygen atoms, tend to retain their coordination sphere. This directional dependence of the Y–O bonding represents an additional restriction to the process of joining particles. Comparing magnesia and yttria as sintering aids, the directional character of Y–O bonding is one of the reasons why yttria performs worse in the sintering of Si_3N_4 compared with magnesia.

4 CONCLUSIONS

The electronic structure is compared and contrasted for the stoichiometric crystals MgO and Y_2O_3. The covalency degree of the metal-to-oxygen bonding, evaluated in terms of the metal orbital admixture to the bonding states, was found to be approximately twice as large for Y_2O_3 compared with MgO. This admixture causes stabilization of the valence states bringing about the two peak structure of the valence band for both oxides. The analysis of the band composition shows increased directional properties of the Y–O bonding compared with Mg–O, corresponding to lowered ability of yttria to join particles in the process of sintering Si_3N_4.

ACKNOWLEDGEMENTS

F. Jollet is thanked for providing the authors with experimental data on Y_2O_3. Thanks are also due to W. Y. Ching for the total DOS curves. The

staff of the Ceramics Department is acknowledged for many stimulating discussions. The work was in part supported by the Slovak Agency for Science (Research Grant No. 4340).

REFERENCES

1. GIACELLO, A. & POPPER, P., *Sci. Ceram.*, **10** (1980) 377.
2. BENGSTRÖM, L. & PUGH, R. J., *J. Amer. Ceram. Soc.*, **72** (1989) 103.
3. COHEN, M. L., LIN, P. J., ROESSLER, D. M. & WALKER, W. C., *Phys. Rev.*, **155** (1966) 992.
4. PANTELIDES, S. T., MICKISH, D. J. & KUNZ, A. B., *Phys. Rev. B*, **12** (1975) 5203.
5. WALCH, P. F. & ELLIS, D. E., *Phys. Rev. B*, **12** (1975) 5920.
6. DAUDE, N., JOUANIN, C. & GOUT, C., *Phys. Rev. B*, **15** (1977) 2399.
7. YAMASHITA, J. & ASANO, S., *J. Phys. Soc. Japan*, **52** (1983) 3506.
8. BUKOWINSKI, M. S. T., *J. Geophys. Res.*, **87** (1982) 303.
9. CHENG, K. J. & COHEN, M. L., *Phys. Rev. B*, **30** (1984) 4774.
10. TAURAIN, O. E., SPRINGBORG, M. & CHRISTENSEN, N. E., *Solid State Commun.*, **55** (1985) 351.
11. KLEIN, B. M., PICKETT, W. E., BOYER, L. L. & ZELLER, R., *Phys. Rev. B*, **35** (1987) 5802.
12. LOBATCH, V. A., KULYABIN, B. E., ZHUKOV, V. P. & MEDVEDEVA, N. I., *Phys. Status Solidi B*, **158** (1990) 239.
13. CAUSA, M., DOVESI, R., PISANI, C. & ROETTI, C., *Phys. Rev. B*, **33** (1986) 1308.
14. SCHWARZ, K., *Phys. Chem. Minerals*, **14** (1987) 315.
15. XU, Y.-N. & CHING, W. Y., *Phys. Rev. B*, **43** (1991) 4461.
16. CHING, W. Y. & XU, Y.-N., *Phys. Rev. Lett.*, **65** (1990) 895.
17. JOLLET, F., NOGUERA, C., THROMAT, N., GAUTIER, M. & DURAUD, J. P., *Phys. Rev. B*, **42** (1990) 7587.
18. HOFFMANN, R., *J. Chem. Phys.*, **39** (1963) 1397.
19. WHANGBO, M.-H. & HOFFMANN, R., *J. Amer. Chem. Soc.*, **100** (1978) 6093.
20. WHANGBO, M.-H., EVAIN, M., HUNGBANKS, T., KERTESZ, M., WIJEYESEKERA, S. D., WILKER, C., ZHENG, C. & HOFFMANN, R., Quantum Chemistry Program Exchange No. 571, Indiana University, 1988.
21. SASAKI, S., FUJINO, K. & TAKEUCHI, Y., *P. Japan. Acad.*, **55** (1979) 43.
22. WYCKOFF, R. W. G., *Crystal Structures*, Chap. 5, p.5. Interscience, New York, 1966,
23. SMRČOK, Ľ., *Cryst. Res. Technol.*, **24** (1989) 607.
24. RAMIREZ, R. & BÖHM, M. C., *Int. J. Quantum Chem.*, **30** (1986) 391.
25. YEE, K. A. & HUGHBANKS, T., *Inorg. Chem.*, **31** (1992) 1620.
26. FIERMANS, L., HOOGEWIJS, R., DE MEYER, G. & VENNIK, J., *Phys. Status Solidi A*, **59** (1980) 569.
27. KOWALCZYK, S. P., McFEELY, F. R., LEY, L., GRITSYNA, V. T. & SHIRLEY, D. A., *Solid State Commun.*, **23** (1977) 161.
28. HOFFMANN, R., *Solids and Surfaces: A Chemist's View of Bonding in Extended Structures*. VCH Publishers, Inc., New York, 1988.
29. HARUYAMA, Y., FUKUTANI, H., AIURA, Y., NISHIHARA, Y., KOMEDA, T., KODAIRA, S., MARUYAMA, T. & KATO, H., *Japan J. Appl. Phys.*, **32** (1993) Suppl. 32.
30. VINCENZINI, P., *Ceramurgia*, **16** (1986) 3 (in Italian).
31. GOGOTSI, Y. G. & LAVRENKO, V. A., *Corrosion of High-Performance Ceramics*. Springer-Verlag, Berlin, 1992.
32. BENCO, Ľ., *Surface Sci.* (submitted for publication).
33. CAUSA, M., DOVESI, R., PISANI, C. & ROETTI, C., *Phys. Rev. B*, **34** (1986) 2939.
34. HOFFMAN, R., *Rev. Mod. Phys.*, **60** (1988) 601.